Vibrational Anharmonicities Revealed by Coherent Two-Dimensional Infrared Spectroscopy

O. Golonzka, M. Khalil, N. Demirdöven, and A. Tokmakoff
Department of Chemistry, Massachusetts Institute of Technology, Cambridge, Massachusetts 02139
(Received 12 October 2000)

Two-dimensional infrared photon echo spectroscopy has been used to describe the anharmonic nuclear potential of two coupled molecular vibrations. The two-dimensional spectrum shows diagonal and off-diagonal features, each composed of two peaks. The splitting between these peaks is directly related to the anharmonicity, while the relative amplitude of the diagonal and off-diagonal features describes the projection angle between interacting dipoles.

DOI: 10.1103/PhysRevLett.86.2154 PACS numbers: 78.47.+p, 42.50.Md, 82.20.Rp

One of the objectives of condensed phase molecular spectroscopy is to characterize the evolution of microscopic structure accompanying time-dependent physical and chemical processes. One approach to accessing this transient structural information is to use vibrational spectroscopy to characterize intramolecular and intermolecular interactions between different nuclear coordinates on a time scale fast compared to structural change. Since vibrational transitions are often associated with well-defined nuclear motions, the orientation of vibrational transition dipole moments can be related to the orientation of the specific chemical bonds, while vibrational transition frequencies reflect the coupling between molecular motions as encoded in the anharmonicity of the nuclear potential. Traditional vibrational spectroscopy is limited in its usefulness in recovering this information; since spectra are congested, lines are broadened by various dynamic or static mechanisms, and overtone and combination bands are obscured. The limitations of these one-dimensional (1D) methods are the motivation for the current development of nonlinear vibrational spectroscopies with higher dimensionality [1–5]. Two-dimensional (2D) vibrational spectra directly arise from anharmonic effects, and therefore are a sensitive probe of molecular couplings. Furthermore, 2D spectra reduce spectral congestion by spreading the resonances into two dimensions, discriminate between dynamic and static spectral broadening mechanisms, and allow relative orientations of coupled vibrations to be probed.

In this Letter, we demonstrate how coherent 2D infrared (IR) spectroscopy can be used to directly extract anharmonic couplings between strongly coupled vibrational modes. 2D Fourier transform vibrational spectroscopy observes the creation and evolution of coherences involving coupled vibrational states, and represents them as a 2D spectrum whose frequency axes describe the preparation and detection period. 2D IR photon echo (PE) spectroscopy is a resonant third-order nonlinear spectroscopy that monitors the evolution of the system during two independent time periods τ_1 and τ_3. This method is derived from IR-PE experiments that have previously been used to study vibrational dynamics of a single coordinate [6]. The nonlinear signal generated by three vibrationally resonant pulsed laser fields $\mathbf{E}_1(k_1)$, $\mathbf{E}_2(k_2)$, and $\mathbf{E}_3(k_3)$, is radiated in the $k_{\mathrm{sig}} = -k_1 + k_2 + k_3$ wave-vector matching direction. After the first pulse $\mathbf{E}_1$, the system propagates in a vibrational coherence during time τ_1. Pulses $\mathbf{E}_2$ and $\mathbf{E}_3$, incident simultaneously, can lead to (i) rephasing of the initial coherence, (ii) excitation of coherences involving other vibrational coordinates, or (iii) excitation of higher lying vibrational coherences. The evolution of the system during the final coherence time τ_3 can be monitored by heterodyne detection or spectral interferometry using a separate local oscillator (LO) field [4–7]. In general, the diagonal peaks in such a spectrum ($-\omega_1 = \omega_3$) contain information about the nuclear potential governing molecular motion along a single vibrational coordinate, whereas the interaction of different vibrational motions is observed as the formation of cross peaks in the 2D spectrum.

One task facing the development of 2D vibrational spectroscopy is relating the placement, shape, and intensity of cross peaks to the strength and mechanism of vibrational coupling. Several interaction mechanisms lead to signals in 2D IR experiments: (i) vibrational anharmonicity due to through-bond and/or through-space electrostatic interactions; (ii) electrical anharmonicity due to nonlinearity of the dipole moment with respect to the vibrational coordinate; and (iii) quantum-number-dependent dephasing dynamics [8]. These types of vibrational nonlinearities have also been identified in the description of 2D Raman spectroscopy [2,9,10]. Previous 2D IR experiments based on frequency-resolved pump-probe spectroscopy have investigated nuclear interactions arising from dipole couplings between amide I vibrations in peptides and proteins [11–13].

To this point, a systematic experimental investigation of the influence of different interaction mechanisms on 2D spectra using a set of well-characterized model compounds is lacking. As a model system of vibrations coupled through mechanical anharmonicity, we study the 2D IR spectrum of the symmetric and asymmetric carbonyl (CO) stretching bands of dicarbonylacetylacetonato rhodium (I) (RDC) [14,15]. The coupling between the symmetric ($\omega_s = 2084\ \mathrm{cm}^{-1}$) and asymmetric ($\omega_a = 2015\ \mathrm{cm}^{-1}$)

 0031-9007/01/86(10)/2154(4)$15.00

CO stretching motions leads to an anharmonic potential that is characterized by the vibrational transitions in Fig. 1. The anharmonic frequency shifts of the overtone spectrum are measured at $\Delta_s = 11\ \mathrm{cm}^{-1}$ and $\Delta_a = 14\ \mathrm{cm}^{-1}$ for the symmetric and asymmetric vibrations, while the frequency of the combination band is redshifted by $\Delta_{sa} = 25\ \mathrm{cm}^{-1}$ with respect to the sum of the fundamental frequencies. Experiments in hexane, where the homogeneous linewidth ($<3\ \mathrm{cm}^{-1}$) is smaller then the strength of the vibrational coupling, allow us to resolve all possible resonances in the 2D experiment. Both eigenstate descriptions [8] and a nonlinear exciton model [3] predict ten well-separated spectral peaks in this experiment, each describing a particular progression of vibrational coherences.

The experiment uses 90 fs mid-IR pulses ($\lambda = 4.9\ \mu$m; $\nu = 2050\ \mathrm{cm}^{-1}$) obtained by difference frequency mixing the signal and idler outputs of a near-IR β-barium borate optical parametric amplifier in a 1 mm $AgGaS_2$ crystal. The collimated IR beam was split into four pulses. One of the beams served as a local oscillator field for heterodyne detection of the third-order signal. The remaining three beams, $\mathbf{E}_1$, $\mathbf{E}_2$, and $\mathbf{E}_3$ (energy 100 nJ each), were arranged into the "box car" geometry and focused to a 150 μm spot in the sample by an $f = 10$ cm parabolic reflector. A stepper motor delay stage was used to control τ_1, the time between $\mathbf{E}_1$ and the time-coincident $\mathbf{E}_2$ and $\mathbf{E}_3$ pulses. The emitted PE signal field was collimated, spatially and temporally overlapped with the LO field, and frequency dispersed in a 190 mm grating monochromator. The interference signal between the LO and signal fields at the detection frequency ω_3 was measured with a HgCdTe detector. The 2D IR data sets were taken by scanning the τ_1 delay for each detection frequency ω_3 and, subsequently, stepping the detection frequency. 2D IR spectra in ω_1 and ω_3 were obtained by Fourier transforming the experimental data along the τ_1 dimension. The polarizations of each of the incident beams, as well as the signal field polarization, were separately controlled with wire grid polarizers.

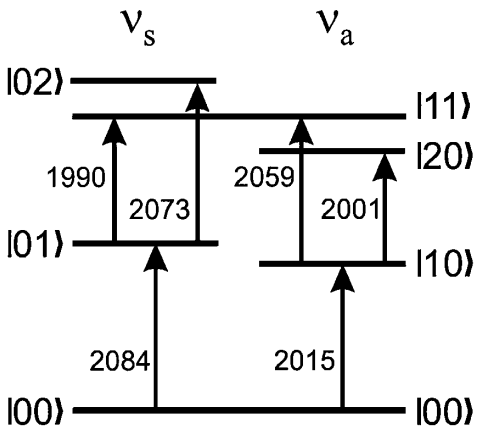

FIG. 1. Energies (in cm^{-1}) of singly excited (one-quantum) and doubly excited (two-quantum) vibrational levels of the symmetric (ν_s) and antisymmetric (ν_a) CO stretch vibrations of RDC. All transition frequencies are within the bandwidth of the IR pulses used in the experiment.

Figure 2 presents the absolute value of the parallel-polarized 2D IR-PE spectrum of RDC in hexane. Each diagonal feature, which arises from processes occurring within one vibrational manifold, consists of two spectral peaks of similar intensity separated along the ω_3 axis by 11 and 14 cm^{-1} for the symmetric and asymmetric vibrations, respectively. The off-diagonal contributions to the 2D spectrum, or cross peaks, represent the processes involving two different vibrational coordinates and therefore contain information pertaining to the coupling of the corresponding vibrations. Similarly to the diagonal features, each of the off-diagonal features is composed of two spectral peaks, which are separated along the ω_3 axis by 25 cm^{-1}. The amplitude of the off-diagonal features is $\sim\frac{1}{3}$ of the amplitude of the diagonal contributions. In addition to the eight relatively strong diagonal and off-diagonal peaks, two single weak peaks were observed at $(\omega_1, \omega_3) = (2015\ \mathrm{cm}^{-1}, 2148\ \mathrm{cm}^{-1})$ and $(2084\ \mathrm{cm}^{-1}, 1928\ \mathrm{cm}^{-1})$ (see insets of Fig. 2).

The response function describing third-order 2D IR experiments is expressed in terms of eight three-time (four-point) correlation functions in the dipole operator, which describe the possible evolution paths of the system. A system of interacting vibrations can be described by a set of singly excited (one-quantum) and doubly excited (two-quantum) states. Destructively interfering pathways

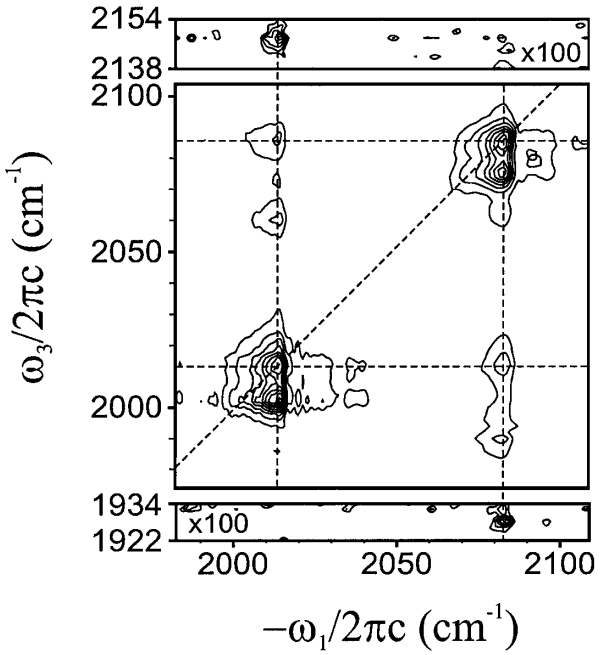

FIG. 2. Absolute value R_{zzzz} 2D IR-PE spectrum of RDC in hexane. The signal in the upper and lower panels is magnified by a factor of 100 to emphasize the weak spectral peaks at $(\omega_1, \omega_3) = (2015\ \mathrm{cm}^{-1}, 2148\ \mathrm{cm}^{-1})$ and $(2084\ \mathrm{cm}^{-1}, 1928\ \mathrm{cm}^{-1})$. Dashed lines indicate the frequencies of the fundamental transitions.

involving these one-quantum and two-quantum states determine the position and strength of each diagonal or off-diagonal feature in the 2D spectrum. In the case of a purely harmonic system, this interference leads to complete quenching of the third-order response. Figure 3 shows an example of two particular interfering pathways contributing to the formation of the off-diagonal features in the 2D spectrum. The evolution of the system in each pathway is identical during the first time period τ_1. During the τ_3 period, the pathway (a) coherence involves a one-quantum state, while the pathway (b) coherence involves a two-quantum state. For uncoupled vibrations, the frequencies during the τ_3 time are identical for both pathways, the pathways destructively interfere, and the signal vanishes. If the two vibrations are coupled, the energy of the two-quantum state describing the combination of these vibrations is shifted with respect to the sum of the energies of the individual one-quantum states by an amount related to the strength of the coupling. The frequencies sampled by such a system during the final coherence time are different for pathways (a) and (b). The resulting absolute value 2D spectrum has two peaks separated along the ω_3 axis by the strength of the vibrational coupling. Similarly, the anharmonicity within the vibrational manifold will be manifested in the 2D spectrum by two opposite-sign peaks split by the strength of the diagonal anharmonicity.

It is clear from the above discussion that a 2D spectrum lends itself to immediate and highly intuitive interpretation and assignment. A single 2D spectrum of RDC carries complete information about the level structure of the singly and doubly excited states of the symmetric and asymmetric stretch manifolds. The anharmonic frequency shifts, $\Delta_s = 11\ \mathrm{cm}^{-1}$ for the symmetric and $\Delta_a = 14\ \mathrm{cm}^{-1}$ for the asymmetric stretch, are measured directly from the separation of the spectral peaks constituting the corresponding diagonal features. The $\Delta_{sa} = 25\ \mathrm{cm}^{-1}$ splitting of the peaks in the off-diagonal features is related to the strength of the coupling between the symmetric and asymmetric

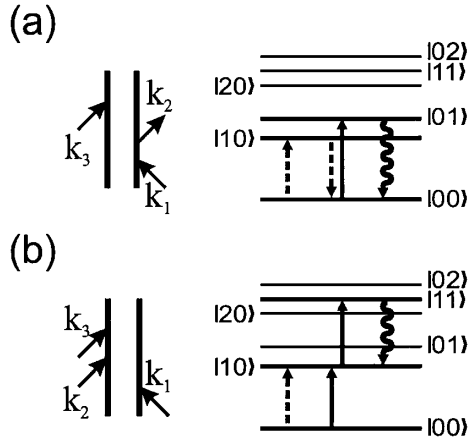

FIG. 3. Feynman diagrams and ladder diagrams representing two competing pathways contributing to the formation of the antidiagonal features in the 2D IR spectrum.

CO vibrational modes. One of the finer demonstrations of the sensitivity of the 2D spectroscopy to the anharmonicities of the nuclear potential is the observation of the weak spectral features at $(\omega_1, \omega_3) = (2015\ \mathrm{cm}^{-1}, 2148\ \mathrm{cm}^{-1})$ and $(2084\ \mathrm{cm}^{-1}, 1928\ \mathrm{cm}^{-1})$. These peaks involve three-quantum transitions between different vibrational manifolds, which are strictly forbidden in a harmonic system.

The characteristics of the nuclear potential V can be deduced from the experimental data by expanding V to third order in the reduced nuclear coordinates Q_s and Q_a:

$$V(Q_s, Q_a) \cong \tfrac{1}{2}\hbar\omega_s^0 Q_s^2 + \tfrac{1}{2}\hbar\omega_a^0 Q_a^2 + \tfrac{1}{6}(g_{sss}Q_s^3 + g_{aaa}Q_a^3 + 3g_{ssa}Q_s^2 Q_a + 3g_{saa}Q_s Q_a^2). \quad (1)$$

Here, ω_i^0 represents the harmonic frequency of mode i. The anharmonicity is described by g_{sss}, g_{aaa}, g_{ssa}, and g_{saa}, the third-order derivatives of the nuclear potential in the equilibrium configuration. In particular, the off-diagonal anharmonicities g_{aas} and g_{ssa} describe the coupling between the Q_s and Q_a coordinates. The experimental values of Δ_s, Δ_a, and Δ_{sa} can be related to the parameters describing the shape of the nuclear potential in a straightforward manner [8]. For RDC in hexane, the corresponding values are $\omega_s^0 = 2108\ \mathrm{cm}^{-1}$, $\omega_a^0 = 2038\ \mathrm{cm}^{-1}$, $g_{sss} = 32\ \mathrm{cm}^{-1}$, $g_{aaa} = 32\ \mathrm{cm}^{-1}$, and $g_{ssa} = g_{saa} = 22\ \mathrm{cm}^{-1}$.

In addition to the anharmonicity of the nuclear potential, the third-order signal can also be due to electrical anharmonicity, the nonlinear dependence of the dipole moment on nuclear coordinate. One effect that will lead to electrical anharmonicity are dipole-induced-dipole interactions, which suggests that 2D IR peak amplitude variations should be sensitive to system-bath interactions. If the dipole moment is expanded in the nuclear coordinates,

$$\mu = \mu^{(0)} + \sum_i \mu_i^{(1)} Q_i + \sum_{i,j} \mu_{ij}^{(2)} Q_i Q_j + \ldots, \quad (2)$$

the nonlinear term, $\mu^{(2)}$, describing deviation of the dipole moment strength from harmonic behavior ($\mu_{1\to 2} = \sqrt{2}\,\mu_{0\to 1}$) causes incomplete cancellation of the one-quantum and two-quantum diagrams. The 2D IR spectral signature of electrical anharmonicity of a system with anharmonic nuclear potential is particularly intuitive: The two peaks that make up a single diagonal or off-diagonal feature will appear with different intensities. In the case of RDC in hexane, the two peaks forming the off-diagonal features are of equal intensity, suggesting that the electrical anharmonicity is small.

Figure 4 presents a simulated absolute value 2D spectrum of RDC for the all-parallel polarization geometry R_{zzzz}. The orientational contributions to the response function were derived by projecting the polarizations of the incident fields onto the directions of the molecular transition dipoles, averaging over all molecular orientations, and

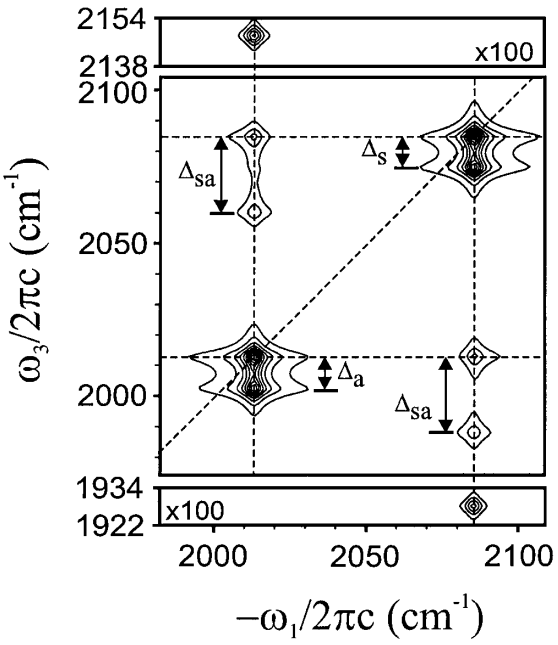

FIG. 4. Simulated absolute value R_{zzzz} 2D IR-PE spectrum of RDC. Dashed lines indicate the frequencies of the fundamental transitions.

accounting for orientational diffusion between interactions with the external fields. The calculation assumes that the transition dipole moments of the symmetric and asymmetric vibrations are perpendicular. The anharmonic coefficients defining the nuclear potential were derived from the anharmonic shifts in Fig. 1. The transition dipole moment strengths of the fundamental transitions of the symmetric and asymmetric vibrations were assumed to be equal. The dipole moments for the transitions into higher lying vibrational states were determined by first calculating the wave functions of the anharmonic two-dimensional oscillator to the first order of perturbation theory, and then evaluating the dipole moment matrix element in the perturbed wave functions. Similarly to the experimental data, the simulated spectrum shows ten peaks, eight of which are combined into characteristic doublets. The approximate $\frac{1}{3}$ intensity ratio of the diagonal of off-diagonal features observed in the experimental spectrum is well reproduced in the simulation and is primarily due to the 90° projection angle between the coupled dipoles.

The remarkable similarities in the observed and calculated spectra clearly demonstrate the efficiency of 2D nonlinear spectroscopy in determining the vibrational anharmonicities and the relative orientation of the interacting dipoles. The shape of the nuclear potential can be linked to the molecular structure by identifying the nature of the local interactions leading to the anharmonicities. Of particular interest as structural probes are the through-space interaction mechanisms, such as dipole-dipole coupling, since they directly relate the strength of the vibrational coupling to the distance and the angle between the interacting groups. Generally, however, the anharmonicities measured in a 2D experiment will include the contributions from both through-space and through-bond coupling mechanisms. Identifying the relative importance of these mechanisms for different molecular systems is of primary interest to development of 2D spectroscopy as a structural tool.

This work was supported by the Office of Basic Energy Sciences, U.S. Department of Energy (DE-FG02-99ER14988), the donors to the ACS-Petroleum Research Fund, and an award by the Research Corporation.

[1] S. Mukamel, Annu. Rev. Phys. Chem. **51**, 691 (2000).
[2] A. Tokmakoff, M. J. Lang, D. S. Larsen, G. R. Fleming, V. Chernyak, and S. Mukamel, Phys. Rev. Lett. **79**, 2702 (1997).
[3] W. M. Zhang, V. Chernyak, and S. Mukamel, J. Chem. Phys. **110**, 5011 (1999).
[4] M. C. Asplund, M. T. Zanni, and R. M. Hochstrasser, Proc. Natl. Acad. Sci. U.S.A. **97**, 8219 (2000).
[5] W. Zhao and J. C. Wright, Phys. Rev. Lett. **84**, 1411 (2000).
[6] K. D. Rector and M. D. Fayer, Int. Rev. Phys. Chem. **17**, 261 (1998).
[7] J. D. Hybl, A. W. Albrecht, S. M. Gallager-Faeder, and D. M. Jonas, Chem. Phys. Lett. **297**, 307 (1998).
[8] M. Khalil and A. Tokmakoff, Chem. Phys. (to be published).
[9] K. Okumura and Y. Tanimura, J. Chem. Phys. **107**, 2267 (1997).
[10] T. Steffen, J. T. Fourkas, and K. Duppen, J. Chem. Phys. **105**, 7364 (1996).
[11] P. Hamm, M. Lim, and R. M. Hochstrasser, J. Phys. Chem. B **102**, 6123 (1998).
[12] P. Hamm, M. Lim, W. F. DeGrado, and R. M. Hochstrasser, Proc. Natl. Acad. Sci. U.S.A. **96**, 2036 (1999).
[13] S. Woutersen and P. Hamm, J. Phys. Chem. B **104**, 11 316 (2000).
[14] J. D. Beckerle, M. P. Casassa, R. R. Cavanagh, E. J. Heilweil, and J. C. Stephenson, Chem. Phys. **160**, 487 (1992).
[15] K. D. Rector, A. S. Kwok, C. Ferrante, A. Tokmakoff, C. W. Rella, and M. D. Fayer, J. Chem. Phys. **106**, 10 027 (1997).